Test Results of the CERN HL-LHC low-β Quadrupole Short Models MQXFS3c and MQXFS4

F.J. Mangiarotti, H. Bajas, G. Ambrosio, M. Bajko, B. Bordini, N. Bourcey, M. Duda, V. Desbiolles, J. Feuvrier, J. Fleiter S. Izquierdo Bermudez, A. Chiuchiolo, A. Devred, P. Ferracin, L. Fiscarelli, M. Mentink, F. Nobrega, K. Pepitone, E. Ravaioli, J. Schmalzle, E. Todesco, J.C. Perez, G. Vallone, G. Willering, M. Yu

Abstract—For the High Luminosity Upgrade of the CERN Large Hadron Collider, lower β* quadrupole magnets based on advanced Nb_3Sn conductors will be installed on each side of the ATLAS and CMS experiment insertion zones. As part of the technological developments needed to achieve the required field gradient of 132.6 T/m within a 150-mm aperture, short length model magnets, named MQXFS, are tested both at the CERN SM18 and FERMI Lab test facilities. The model magnets rely on two types of Nb_3Sn conductors (RRP and PIT) and on an innovative bladders and keys design to provide mechanical support against the Lorentz forces.

In 2016 and 2017, the powering tests of the first two models MQXFS3 (RRP) and MQXFS5 (PIT) proved that nominal performance (16.5 kA) could be reached with excellent memory of the quench current after thermal cycle. However both magnets showed a slow training behavior with clear observations of voltage disturbances before the quench. Besides MQXFS5 only could reach ultimate current (17.9 kA) whereas erratic behavior was observed on MQXFS3 due to conductor local degradation at the head of one of the coil.

In 2018, this limiting coil was changed and the applied azimuthal pre-stress increased. If ultimate current could then be reached, no stable current could be maintained due to identified defect on the outer layer of the new coil.

Finally the outcome of the test of the new model MQXFS4, featuring the final RRP conductors that will be used for the series production and variation on the inner layer quench heater designs are here reported in details.

Index Terms—Nb_3Sn , low beta quadrupole, quench, Superconducting Magnets.

I. INTRODUCTION

IN the framework of the High Luminosity LHC project (HL-LHC) at CERN it is planned to replace the dipoles, quadrupoles and corrector magnets near the main experiments ATLAS and CMS with larger aperture magnets [1]. In particular, the NbTi inner triplet quadrupoles will be replaced by Nb_3Sn quadrupoles, nicknamed MQXF. The characteristic parameters of the present and future inner triplet magnets are summarized in Table I; the cross section of the MQXF magnets is shown in Fig. 1.

F.J. Mangiarotti, H. Bajas, M. Bajko, B. Bordini, N. Bourcey, V. Desbiolles, J. Feuvrier, J. Fleiter S. Izquierdo Bermudez, A. Chiuchiolo, A. Devred, P. Ferracin, L. Fiscarelli, M. Mentink, E. Ravaioli, E. Todesco, J.C. Perez, G. Willering are with CERN, CH-1211, Geneva, Switzerland (email: franco.julio.mangiarotti@cern.ch).
G. Ambrosio, F. Nobrega, M. Yu are with FNAL, Batavia, IL 60510 USA.
M. Duda is with IFJ PAN, Krakow, Poland and CERN, Geneva, Switzerland
K. Pepitone is with Uppsala University, 75105 Uppsala, Sweden.
J. Schmalzle is with BNL, Upton, NY 11973-5000, USA.
G. Vallone is with LBL, Berkeley, CA 94720, USA.
Manuscript received XXX.

TABLE I
SUMMARY OF THE CHARACTERISTIC PARAMETERS OF THE INNER TRIPLET MAGNETS IN LHC AND HL-LHC [2], [1]

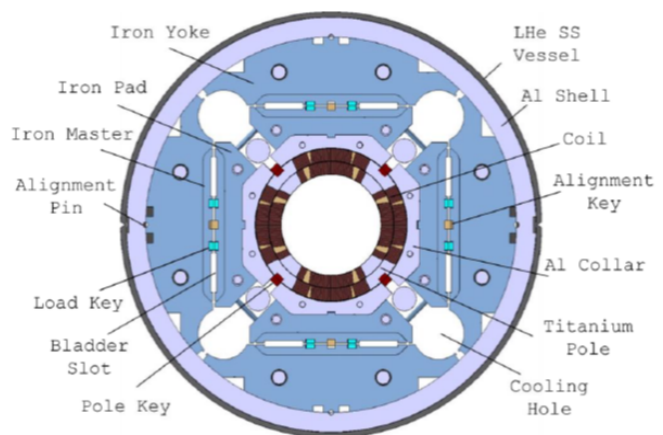| Parameter	Current LHC magnets		HL-LHC magnets	
Nickname	MQXA	MQXB	MQXFA	MQXFB
Position in lattice	Q1, Q3	Q2a, Q2b	Q1, Q3	Q2a, Q2b
Superconductor	NbTi	NbTi	Nb_3Sn	Nb_3Sn
Manufacturer	KEK	FNAL	LARP	CERN
Aperture	70 mm	70 mm	150 mm	150 mm
Nominal gradient	215 T/m	215 T/m	133 T/m	133 T/m
Nominal peak field	8.6 T	7.7 T	11.4 T	11.4 T
Magnetic length	6.37 m	5.5 m	2×4.2 m	7.15 m

Fig. 1. Cross section of the MQXF magnets.

The development program for the new triplet magnets includes the construction and test of five short models with the final design, called MQXFS. The first short model MQXFS1 was tested at FNAL in 2015 [3], [4]. The second and third models, MQXFS3 and MQXFS5, were tested at CERN in 2016-2017 [5]. As the performance of MQXFS3 was limited by one coil, it was decided to disassemble this magnet and re-assemble it with a spare coil; this new magnet was tested again as MQXFS3c in 2017-2018. A fourth model magnet, MQXFS4, was built and tested at CERN in 2018. In this paper we summarize the tests results of MQXFS3c and MQXFS4, and compare them with the previously tested models.

TABLE II
COIL DETAILS OF MQXFS3C AND MQXFS4

Magnet	Coil	Manufacturer	Strand	I_{ss} at 1.9 K
MQXFS3c	8	LARP	RRP 108/127	21.3 kA
	105	CERN	RRP 132/169	
	106	CERN	RRP 132/169	
	107	CERN	RRP 132/169	
MQXFS4	108	CERN	RRP 108/129	22.0 kA
	109	CERN	RRP 108/129	
	110	CERN	RRP 108/129	
	111	CERN	RRP 108/129	

II. SHORT MODEL CONSTRUCTION AND ASSEMBLY FEATURES

In Table II the coils used in magnets MQXFS3c and MQXFS4 are named, with their short sample limit (I_{ss}) and their strand architecture.

A. MQXFS3c

After the limitation observed in MQXFS3 in coil 7 [5], the magnet was fully disassembled. Coil 8, a new coil also manufactured by LARP, was installed in its place, and coils 105 and 106 swapped their location physically and in the electrical circuit. The magnet was then loaded to 140 MPa, aiming to avoid azimuthal unloading up to ultimate current at 1.9 K.

B. MQXFS4

MQXFS4 is assembled out of four coils manufactured at CERN. These coils have the final RRP conductor that will be used for the series production. The magnet was loaded to near 110 MPa azimuthally and 1.2 kN axially. After a first test the magnet assembly MQXFS4a was unloaded axially to introduce a beam screen, and it was reassembled to the same force level as MQXFS4b.

III. TEST PLAN AND FEATURES

A. Magnet instrumentation

All coils are instrumented with 8 voltage taps in each of their two layers, for a total of 64 voltage taps in each magnet. A schematic drawing of the location of the voltage taps is shown in Fig. 2. In addition, the magnet assemblies are instrumented with 32 strain gages, to monitor the strain on the shell, the coils and the tie rods. MQXFS4 also has Fiber Bragg Grating sensors, to measure the strain on the magnet shell [6]. The strain measurements on the magnets are discussed in another paper [7].

B. Magnet protection

The magnet quench detection scheme was described in [5]. For magnet protection, the same three mechanisms used for MQXFS3a-b and MQXFS5 were used: external dump resistor, quench heaters and coupling-loss induced quench (CLIQ) [8], [9]. During training of MQXFS3c CLIQ was not used. The
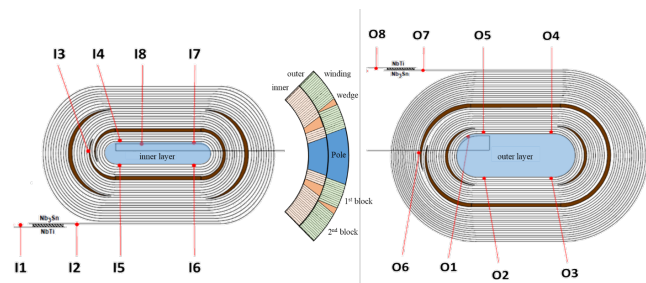

Fig. 2. Schematic drawing of the voltage taps location in MQXFS magnets.

training of MQXFS4 was done with the configuration that better represents the baseline in terms of protection: using CLIQ and outer layer quench heaters, without the external dump.

Both magnets also had additional tests with varying protection schemes to study the effectiveness of these systems. A brief overview of these results is given in the following sections; a more in-depth analysis will be done in the near future.

C. Electrical insulation tests

Standard electrical insulation tests are always performed at the CERN SM18 test facility, both with the magnet in air at room temperature and in liquid helium at 4.5 or 1.9 K. The HL-LHC target test values are defined in [10], and the acceptance criterion is given as a maximum of 10 μA leak current after 30 s of voltage exposure. The test results are summarized in Table III.

MQXFS3c passed the electrical insulation tests up to the test facility target values, as it was tested before the definition of the HL-LHC target values. MQXFS4 passed the tests up to the HL-LHC target values at warm, but it did not pass them at cold. As the maximum voltage during operation would be lower than the maximum voltage at which the insulation test passed, it was deemed safe to continue with the tests.

In addition to the standard electrical insulation tests, in MQXFS3c a set of non-standard tests were done during a third cooldown to qualify the strength of the heater to coil insulation. At three temperature steps (80, 150 and 280 K) the electrical insulation strength in helium gas of the quench heaters to the magnet was tested. With the exception of one heater that was damaged between cooldown #2 and #3, the strength was up to the level of the test facility. These results are summarized in Table IV.

D. Test procedure

The magnets training was done in a superfluid helium bath at 1.9 K, powering with a nominal test ramp rate of 20 A/s as described in [5]. The training was finished once the quench current did not significantly change after several quenches; if the maximum test current is reached before this quench current "plateau", the training is interrupted. Afterwards, other tests at 1.9 K are done, such as ramp rate studies or provoked quenches. Then the quench current is checked again in a liquid helium bath at 4.5 K, and if necessary further tests are done.

TABLE III
STANDARD ELECTRICAL INSULATION TESTS IN MQXFS3C AND
MQXFS4, VALUES IN KV. THE TARGET VALUE IS DESCRIBED IN [10].
"OK" MEANS THE TEST PASSED TO THE LEVEL SPECIFIED, "NOK"
MEANS IT DID NOT. "RT" CORRESPONDS TO TESTS AT ROOM
TEMPERATURE IN AIR.

	Coil-Ground		Coil-Heaters	
	Target	Test	Target	Test
MQXFS3c				
RT before test	3.7	OK: 3.7	3.7	OK: 3.0
In LHe #1	1.8	OK: 1.0	2.3	OK: 1.0
RT after test	0.4	OK: 1.0	0.5	OK: 1.0
In LHe #2	1.8	OK: 1.0	2.3	OK: 1.0
RT after test	0.4	OK: 1.0	0.5	OK: 1.0
MQXFS4a				
RT before test	3.7	OK: 3.7	3.7	OK: 3.0
In LHe	1.8	NOK: 1.0	2.3	NOK: 1.8
RT after test	0.4	OK: 1.0	0.5	OK: 1.0
MQXFS4b				
RT before test	0.4	OK: 1.0	0.5	OK: 0.5
In LHe	1.8	NOK: 1.5	2.3	NOK: 1.9

TABLE IV
SPECIAL ELECTRICAL INSULATION TESTS IN MQXFS3C, THIRD
COOLDOWN. THE RESULTS SHOWN CORRESPOND TO THE HIGHEST
VOLTAGE THAT ALL TESTED HEATERS PASSED AT EACH TEMPERATURE.

Temperature	Voltage	Leak current	Resistance
[K]	[kV]	[nA]	[GΩ]
80	1.5	1.7	894
150	1.0	1.5	699
280	0.8	11	77

IV. MAGNET PERFORMANCE

A. Training

The training curve of MQXFS3 is presented in Fig 3. During the tests of MQXFS3a-b, degradation in coil 7 limited the quench current at 1.9 K and at the nominal test ramp rate of 20 A/s at around 16.7 kA [5]. In MQXFS3c, after changing coil 7 for coil 8, the quench current at 1.9 K and at 20 A/s was limited on coil 106 at a much lower value: around 15.6 kA. At 200 A/s, however, the four coils of the magnet continued training, up to a maximum current of around 18.1 kA, higher than the 17.6 kA reached in MQXFS3b at this ramp rate. The quench current at 4.5 K and 20 A/s (17.4 kA) is slightly lower than that of MQXFS3b (17.6 kA).

The training curve of MQXFS4 is presented in Fig 4. MQXFS4 reached the nominal current at 1.9 K after only one quench, and the ultimate current after 5 quenches. No coil showed a limitation that prevented the magnet for further training; the tests were stopped at 200 A above ultimate current (18.1 kA) to avoid the risk of unnecessary damage to the magnet. After a thermal cycle, the magnet reached 18.1 kA without any quench. Tests at 4.5 K were not done due to time constraints.
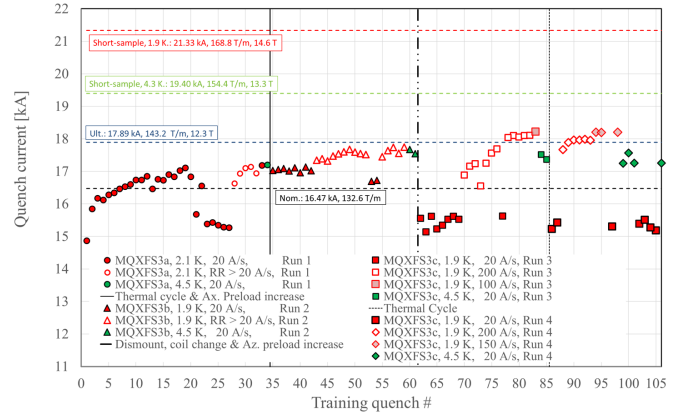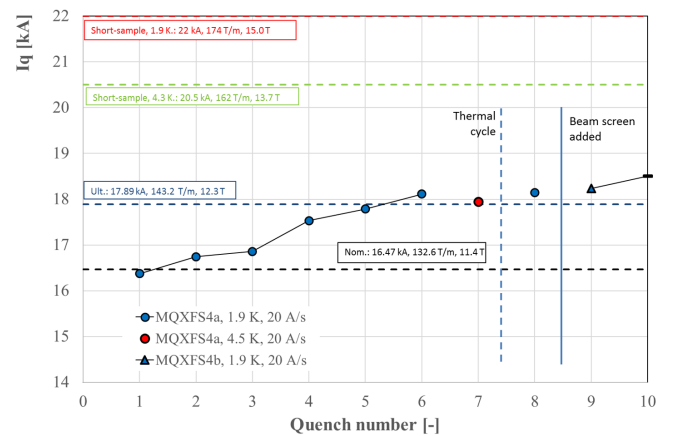

Fig. 3. Training curve of MQXFS3a–c.

Fig. 4. Training curve of MQXFS4.

B. Ramp rate studies

The ramp rate dependency of MQXFS3 and MQXFS4 is shown in Fig 5. MQXFS3c shows a maximum quench current at 150 A/s at 1.9 K. Below that level, the quench current is limited by degradation in the outer layer of coil 106. At 250 A/s and above, the magnet quenches in the second block of the inner layer of coil 8. At 4.5 K the quench current decreases monotonically with increasing ramp rate. The magnet behavior at high ramp rates is similar, however at ramp rates up to 150 A/s the quench location is the pole turn of the outer layer of coil 107. At 50 A/s and below, the quench current at 4.5 K is higher than at 1.9 K.

Since the training was not finished for MQXFS4, we can only analyze its ramp rate dependency up to 18.1 kA. Below 200 A/s the magnet does not quench; at 400 A/s the magnet quenches at 17.1 kA. The quench at 400 A/s occurs simultaneously in several segments in coils 109 and 111.

C. Other cold tests

The residual resistance ratio (RRR) of the coils in the magnets was measured during the warm up. The measurement is done from the transition temperature (around 18 K) up to room temperature. The values reported in Table V are extrapolated to the standard values of 4 K to 293 K.
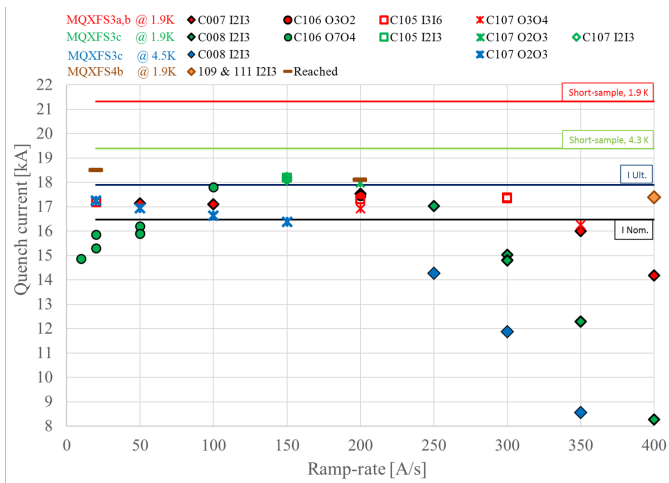
Fig. 5. Ramp rate dependency of the quench current in MQXFS3 and MQXFS4.

Fig. 6. Comparison of the training of the four MQXF model magnets. Note that the horizontal axis is in logarithmic scale.

B. Performance comparison of the four model magnets

A comparison of the training of the four MQXF model magnets is shown in Fig. 6. MQXFS4 presents the fastest training to both nominal and ultimate current so far. MQXFS3c reached ultimate current with a much higher number of quenches than the other models, and it did so with a ramp rate of 200 A/s – ten times larger than the others. All magnets show a very good training memory after a thermal cycle.

TABLE V
RESIDUAL RESISTANCE RATIO (RRR) AND SPLICES RESISTANCE (R) OF
THE COILS. NO DATA MARKED AS N/D.

Magnet	MQXFS3c				MQXFS4			
Coil	8	105	106	107	108	109	110	111
$RRR_{293K/4K}$	180	154	158	137	170	160	165	165
R_{I1-I2} [nΩ]	N/D	0.10	0.31	0.19	0.18	N/D	N/D	0.40
R_{O7-O8} [nΩ]	N/D	0.19	0.16	0.14	N/D	0.39	0.43	0.43

Each coil has two NbTi–Nb$_3$Sn splices, marked as I1-I2 and O7-O8 in Fig 2. These splices resistance has been calculated by measuring the voltage across these voltage taps at several current levels. The resistance values are summarized in Table V.

V. DISCUSSION

A. Quench current limitation in MQXFS3c due to degradation

From the quench current limitation described in the previous section, we identified three locations that are degraded: (a) 106 O4-O7 at 1.9 K and below 150 A/s, (b) 8 I2-I3 at 1.9 K and 4.5 K at or above 250 A/s, and (c) 107 O2-O3 at 1.9 K between 150 and 200 A/s and at 4.5 K at or below 150 A/s.

The degradation in location (a) appeared after the coil change MQXFS3b to MQXFS3c. Location (b) is in the new coil in MQXFS3c. A limitation in location (c) was not observed in MQXFS3b: at 4.5 K and 20 A/s the quench in a different location and at a higher current; at 1.9 K and 200 A/s the quench current was slightly lower and in a different location. Ramp rate studies at 4.5 K were not done for MQXFS3b.

Degradation in locations (a) and (c) seem to originate either from the coil change process or from the subsequent increase of the azimuthal pre-load in the magnet. As coil 8 has not been tested before, degradation in location (b) could originate from the magnet assembly process, or from the coil manufacturing process itself.
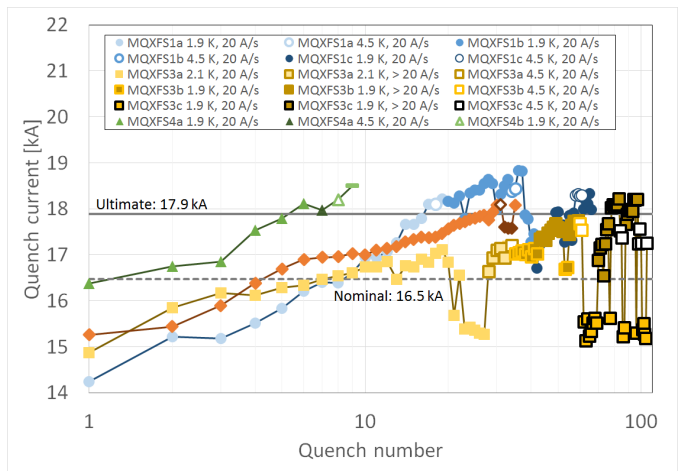
VI. CONCLUSION

A new low-beta quadrupole short model magnet magnet assembly, MQXFS3c, and a fully new magnet, MQXFS4, have been tested at the CERN magnet facility SM18. The results are summarized below.

MQXFS3c shows some degradation at nominal ramp rate, compared to MQXFS3b, however at higher ramp rates it reached a quench current above ultimate for the first time.

The ramp rate studies in MQXFS3c show three locations with degradation. Two of those locations are in already tested coils, and the degradation seems to originate from the coil change process. The other degraded location is in the new coil.

MQXFS4 reached nominal current after one quench and ultimate current after 5 quenches. It had great training memory after a thermal cycle, reaching ultimate current without any quench. At 200 A/s it does not quench up to ultimate current.

Besides training, other tests have been performed. RRR, inductance and splice resistance measurements have been performed, with results as expected. Standard electrical insulation tests have been performed as usual, with good results in the case of MQXFS3c and below the expected in the case of MQXFS4 at cold. Additional electrical insulation tests were performed in MQXFS3c in helium gas.

REFERENCES

[1] E. Todesco, H. Allain, G. Ambrosio, G. Arduini, F. Cerutti, R. D. Maria, L. Esposito, S. Fartoukh, P. Ferracin, H. Felice, R. Gupta, R. Kersevan, N. Mokhov, T. Nakamoto, I. Rakno, J. M. Rifflet, L. Rossi, G. L. Sabbi, M. Segreti, F. Toral, Q. Xu, P. Wanderer, and R. van Weelderen, "A first

baseline for the magnets in the high luminosity lhc insertion regions," *IEEE Transactions on Applied Superconductivity*, vol. 24, no. 3, pp. 1–5, June 2014.

[2] O. S. Brüning, P. Collier, P. Lebrun, S. Myers, R. Ostojic, J. Poole, and P. Proudlock, "Lhc design report," CERN, Tech. Rep., 2004.

[3] G. Chlachidze, G. Ambrosio, M. Anerella, R. Bossert, E. Cavanna, D. W. Cheng, D. R. Dietderich, J. DiMarco, H. Felice, P. Ferracin, A. K. Ghosh, P. Grosclaude, M. Guinchard, A. R. Hafalia, E. F. Holik, S. I. Bermudez, S. T. Krave, M. Marchevsky, A. Nobrega, D. Orris, H. Pan, J. C. Perez, S. Prestemon, E. Ravaioli, G. Sabbi, T. Salmi, J. Schmalzle, S. E. Stoynev, T. Strauss, C. Sylvester, M. Tartaglia, E. Todesco, G. Vallone, G. Velev, P. Wanderer, X. Wang, and M. Yu, "Performance of the first short model 150-mm-aperture nb3sn quadrupole mqxfs for the high-luminosity lhc upgrade," *IEEE Transactions on Applied Superconductivity*, vol. 27, no. 4, pp. 1–5, June 2017.

[4] S. Stoynev, G. Ambrosio, M. Anerella, R. Bossert, E. Cavanna, D. Cheng, D. Dietderich, J. DiMarco, H. Felice, P. Ferracin, G. Chlachidze, A. Ghosh, P. Grosclaude, M. Guinchard, A. R. Hafalia, E. F. Holik, S. I. Bermudez, S. Krave, M. Marchevsky, A. Nobrega, D. Orris, H. Pan, J. C. Perez, S. Prestemon, E. Ravaioli, G. Sabbi, T. Salmi, J. Schmalzle, T. Strauss, C. Sylvester, M. Tartaglia, E. Todesco, G. Vallone, G. Velev, P. Wanderer, X. Wang, and M. Yu, "Summary of test results of mqxfs1the first short model 150 mm aperture nb3sn quadrupole for the high-luminosity lhc upgrade," *IEEE Transactions on Applied Superconductivity*, vol. 28, no. 3, pp. 1–5, April 2018.

[5] H. Bajas, G. Ambrosio, A. Ballarino, M. Bajko, B. Bordini, N. Bourcey, D. W. Cheng, M. Cabon, A. Chiuchiolo, G. Chlachidze, H. Felice, L. Fiscarelli, M. Juchno, S. I. Bermudez, M. Guinchard, J. Kopal, F. Lackner, M. Marchevsky, F. Nobrega, H. Pan, J. C. Perez, H. Prin, E. Ravaioli, L. Rossi, G. Sabbi, S. S. Tavares, J. Steckert, S. Stoynev, E. Todesco, G. Vallone, P. Wanderer, X. Wang, and M. Yu, "Test result of the short models mqxfs3 and mqxfs5 for the hl-lhc upgrade," *IEEE Transactions on Applied Superconductivity*, vol. 28, no. 3, pp. 1–6, April 2018.

[6] A. Chiuchiolo, H. Bajas, M. Bajko, N. Bourcey, M. Cabon, P. Ferracin, P. Grosclaude, M. Guinchard, J. C. Perez, and G. Vallone, "Strain measurements with fiber bragg grating sensors in the short models of the hilumi lhc low-beta quadrupole magnet mqxf," *IEEE Transactions on Applied Superconductivity*, vol. 28, no. 4, pp. 1–5, June 2018.

[7] G.Vallone *et al.*, "Summary of the mechanical performances of the 1.5m long models of the nb3sn low- quadrupole mqxf," *IEEE Transactions on Applied Superconductivity*, under review.

[8] E. Ravaioli, V. I. Datskov, C. Giloux, G. Kirby, H. H. J. ten Kate, and A. P. Verweij, "New, coupling loss induced, quench protection system for superconducting accelerator magnets," *IEEE Transactions on Applied Superconductivity*, vol. 24, no. 3, pp. 1–5, June 2014.

[9] E. Ravaioli, "Cliq," Ph.D. dissertation, University of Twente, 2015.

[10] F. M. Camara and F. R. Mateos, "Hl-lhc electrical design criteria for the it magnets," CERN, Tech. Rep. EDMS 1963398, 2018.